Global Journal of Pure and Applied Mathematics.
ISSN 0973-1768 Volume 14, Number 10 (2018), pp. 1389–1406

http://www.ripublication.com/gjpam.htm

Modeling Traffic Flow on Multi-Lane Road: Effects of Lane-Change Manoeuvres Due to an On-ramp

William Kuria Ndungu

Department of Pure and Applied Mathematics,
Jomo Kenyatta University of Agriculture and Technology,
P.O Box 62000-00200, Nairobi, Kenya.

Mark E. M. Kimathi

Department of Mathematics, Statistics and Actuarial Sciences,
Machakos University, P.O Box 136-90100, Machakos, Kenya.

David Mwangi Theuri

Department of Pure and Applied Mathematics,
Jomo Kenyatta University of Agriculture and Technology,
P.O Box 62000-00200, Nairobi, Kenya.

Abstract

Traffic breakdown is the main cause of vehicle traffic congestion in our multi-lane roads due to highway bottlenecks such as lane-drops, on and off-ramps. In this study the three phase traffic flow theory is outlined and the nature of traffic breakdown at highway bottlenecks explained. A multi-lane macroscopic traffic flow model of Aw-Rascle type is derived from kinetic traffic flow model which expresses the lane change term explicitly. For simulation of this traffic congestion, we consider a highway with three traffic lanes that has a stationary bottleneck (on-ramp). The model equations for each lane are solved numerically using finite volume method (Godunov scheme), whereby the Euler's method was used for the source term. The results of simulation near and within the on-ramp is presented in form of graphs and space-time plots. These results indicate that vehicle lane-change manoeuvres lead to heavy traffic breakdown and congestion on the lane adjacent to the bottleneck compared to the other lanes. This is due to the merging of vehicles from on-ramp prompting the following vehicle moving in the adjacent lane to either slow down

upon reaching the disturbance region or change to the other lanes before they reach the merging zone.

AMS subject classification:
Keywords: Traffic breakdown, On-ramp, Godunov scheme, Merging zone, Lane-change manoeuvre.

1. Introduction

Vehicular traffic congestion is a condition on transport networks that occurs when a volume of traffic generates demand for space greater than the available road capacity, and is a major problem experienced in our roads within urban areas. It exhibits a spatiotemporal traffic pattern which is a distribution of traffic flow variables (speed and density) in space and time. One way of solving this problem is to add more lanes on the existing roadways to increase our road capacity. Sometimes this remedy is restricted by lack of space, resources, environments and bad governance. Therefore we need to have a proper understanding of empirical traffic congestion for an effective traffic management, control and organization. Traffic flow theories and models which describe in a precise mathematical way the vehicle to vehicle, vehicle and infrastructure interactions are required to explain the real cause of traffic congestion. One of the main causes of traffic congestion in our road network is traffic breakdown in an initially free flowing traffic near the bottlenecks, Kerner [1]. Traffic breakdown is described as an abrupt decrease in average vehicle speed in a free traffic flow to a lower speed in congested traffic and usually occurs at highway bottlenecks such as lane-drops, road constructions, accident area, weaving section, on and off ramps etc. This traffic breakdown is due to dynamic competition of the "speed adaptation effect" which describes a tendency of traffic towards synchronized flow and the "over-acceleration effect" describing a tendency of traffic towards free flow. Traffic congestion may lead to various negative effects to motorists such as wasting time, delays in arrivals for employment and education, fuel wastage, wear and tear etcetera. However, traffic congestion has the advantage of encouraging travelers to re-time their trips early enough so that valuable road space is in full use for the most number of hours per day. Thus the need to develop macroscopic traffic flow models which describes the traffic flow dynamics by averaging vehicle density, velocity and flow rate. According to Kerner [1], vehicular traffic is a complex dynamic process associated with the spatiotemporal behavior of many particles systems. This is mainly due to nonlinear interactions between travel decision behavior, routing of vehicles in traffic network and traffic congestion occurrence within the road network. Normally traffic flow is considered to be either in free flow or congested state but the later exists in two different phases i.e. synchronized flow and wide moving jams. Lighthill and Whitman [2] started the macroscopic modeling of vehicular traffic by considering the equation of continuity for traffic density (ρ) and closing the equation by an equilibrium assumption on the mean velocity (u). Later Payne [3] introduced an additional momentum equation for the mean velocity in analogy to fluid dynamics to the above mentioned

model. These macroscopic models predicted that if in front of a driver traveling at a certain speed and the vehicle density is increasing but the vehicles ahead are faster, then the driver will slow down. However a common observation is that a reasonable driver will obviously accelerate when the traffic in front is moving at higher speed than he is. This inconsistency was pointed out by Daganzo [4] and was resolved by Aw and Rascle [5] who developed a new heuristic macroscopic model from kinetic equations describing the entire situation correctly. Klar and Wegener [6] derived macroscopic traffic equations from the underlying kinetic models by considering a highway with N lanes involving the vehicle interactions when changing lanes to either left or right. Ahmed [7] found that mandatory lane-change processes exhibit different behavior compared to the immediate lane-changing models of Hoogendoorn [8] who included driver behavior. That is, mandatory lane-change occurs at bottlenecks where the vehicles are forced to change to a fixed target lane and lead to traffic breakdown due to the increase of traffic demand on the road capacity. The later happens when a vehicle approaches a slower one, seeks for a sufficient gap in its target lane and change lanes immediately the gap is available. Earlier traffic flow theories and models missed the discontinuous character of probability of passing introduced in the three-phase traffic theory of Kerner [1]. Thus they could not explain the traffic breakdown at the highway bottleneck as observed in real traffic data. In this research we will use the kinetic traffic flow model of Klar and Wegener [6] which expresses the lane-change term explicitly from pure anticipation term to develop the macroscopic traffic flow model equations. According to Helbing [9], well-defined criteria for a good traffic flow model should contain only a few parameters and variables which are easy to observe, and the measured values are realistic to suit our macroscopic traffic flow model. Furthermore a good traffic model should reproduce all known features of traffic flow like localized jams and all transition states of traffic congestion and this descriptions fit our new multi-lane macroscopic traffic flow model. Thus vehicle lane-change manoeuvres can maintain free traffic flow, lead to traffic breakdown or emergence of wide moving jam near the bottlenecks and this is what our research is based on.

2. Mathematical Formulation

2.1. The Kinetic Traffic Multi-lane Flow Model

The kinetic traffic flow model is described by use of the distribution functions of velocity of vehicles in traffic flow. We consider a highway with N lanes numbered by $\alpha = 1, \ldots, N$. Letting $f_\alpha(x, v)$ denote a single car distribution function which describes the number of cars at x with velocity v on lane α. If $F_\alpha(x, v)$ denote the probability distribution in v of cars at x i.e. $f_\alpha(x, v) = \rho_\alpha(x) F_\alpha(x, v)$, $F_\alpha^+(v_+; h, v, x)$ denote the probability distribution in v_+ of the leading cars at distance h for cars at x with velocity v, and $Q_\alpha(h; v, x)$ denote the probability distribution of leading cars in h for a car at x with velocity v, then;

$$f_\alpha(x, v, h, v_+) = F_\alpha^+(v_+; h, v, x)\, Q_\alpha(h; v, x)\, f_\alpha(x, v) \tag{1}$$

Assuming the leading vehicles are distributed according to the probability $F_\alpha(x,v)$ at $x+h$ i.e $F_\alpha^+(v_+;h,v,x) = F_\alpha(x+h,v_+)$ and $Q_\alpha(h;v,x) = q_\alpha(h;v,f_\alpha(x,v))$ then

$$f_\alpha(x,v,h,v_+) \sim q_\alpha(h;v,f_\alpha(x,v))\, F_\alpha(x+h,v_+)\, f_\alpha(x,v) \tag{2}$$

Here the kinetic equation for the distribution functions $(f_1,\ldots,f_N)$ on N lanes is obtained by finding the kinetic interaction operators, Klar and Wegener [6] i.e the Gain (G) and Loss (L) operators:

$$\partial_t f_\alpha + v\partial_x f_\alpha = C_\alpha^+(f_1,\ldots,f_N) = \left(G_B^+ - L_B^+\right)(f_{\alpha-1},f_\alpha,f_{\alpha+1})$$

$$+\left(G_A^+ - L_A^+\right)(f_\alpha) + \left[G_R^+(f_\alpha,f_{\alpha+1},f_{\alpha+2}) - L_R^+(f_\alpha,f_{\alpha+1})\right]$$

$$+\left[G_L^+(f_{\alpha-1},f_\alpha) - L_L^+(f_{\alpha-1},f_\alpha,f_{\alpha+1})\right] \tag{3}$$

Taking $\rho_\alpha = \int_0^w f_\alpha(x,v)\,dv$, $f_\alpha = \rho_\alpha F_\alpha$ and $q_X(v,f_\alpha) = q(H_X(v),v,f_\alpha)$ where $H_X(v)$; $X = B,A$ is the threshold for braking and acceleration respectively. The left hand side of the partial differential equation (3) describes the continuous dynamics of the phase-space density (PSD) due to the motions of traffic flow while the right hand side describes the discontinuous changes of this function due to lane-changing, acceleration and deceleration. Defining probability P_Y, $Y = L,R$ for a lane change to either left (L) or right (R) and using the convention $P_R(v,f_{N+1}) = P_L(v,f_0) = 0$, then the gain and loss terms in equation (3) can be approximated as follows, taking lane α as the considered lane:

Remark 2.1. In this study the traffic flow regulation is based on keep left lane rule for slow moving vehicles unless overtaking. The following figure (1) shows the multi-lane highway under consideration in our traffic flow modeling. The arrows indicate the gain and loss interaction terms due to vehicle changing lanes to their target lanes.

Gain and Loss Due to Lane Changing to the Right
A vehicle will change lane to the right if the braking line is reached and a lane change is possible with a probability P_R, resulting to the following vehicle interactions:
(a) *Gain term from the right (* G_R^+*) defined as;*

$$G_R^+(f_\alpha,f_{\alpha+1},f_{\alpha+2})$$

$$= \int_{\hat{v}_->v} P_L(v,\rho_\alpha)\left[1 - P_R\left(\hat{v}_-,\rho_{\alpha+2}\right)\right]|v-\hat{v}_-|q_B\left(\hat{v}_-,\rho_{\alpha+1}\right)$$

$$\times\rho_{\alpha+1}\delta u_{\alpha+1}^-\left(\hat{v}_-\right)\delta u_{\alpha+1}(v)\,d\hat{v}_- \tag{4}$$

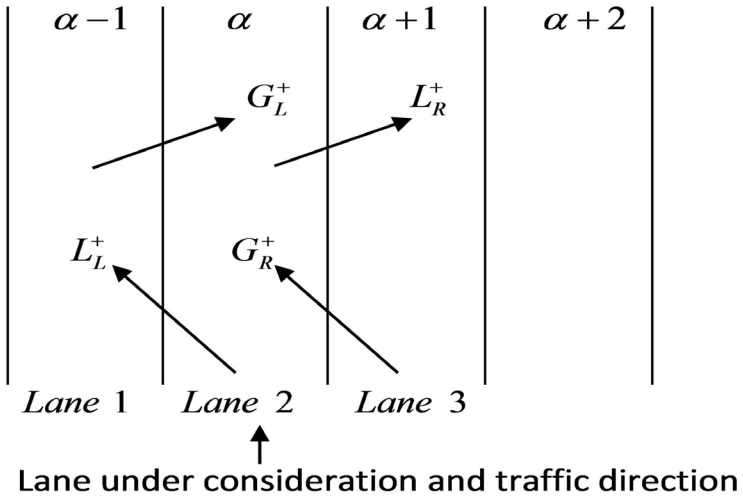

Figure 1: Section of the multi-lane highway showing the kinetic traffic interaction operators due to lane-changing manoeuvres.

(*b*) *Loss term to the right* $\left(L_R^+\right)$ *defined as:*

$$L_R^+ \left(f_\alpha, f_{\alpha+1}\right)$$

$$= \int_{v>\hat{v}_+} P_R\left(v, f_{\alpha+1}\left(x,v\right)\right) |v-\hat{v}_+| q_B\left(H_B\left(v\right), f_\alpha\left(x,v\right)\right) \rho_\alpha \delta u_\alpha\left(v\right) \delta u_\alpha^+\left(\hat{v}_+\right) d\hat{v}_+$$

$$= \int_{v>\hat{v}_+} P_R\left(v, \rho_{\alpha+1}\right) |v-\hat{v}_+| q_B\left(H_B\left(v\right), \rho_\alpha\right) \rho_\alpha \delta u_\alpha\left(v\right) \delta u_\alpha^+\left(\hat{v}_+\right) d\hat{v}_+ \qquad (5)$$

Gain and Loss Due to Lane Changing to the Left
A vehicle will change lane to the left if it reaches the braking line and is not able to overtake using the right lane. This yields the vehicle interactions defined below:
(*a*) *Gain term from the left lane* (G_L^+) *defined as*:

$$G_L^+ \left(f_{\alpha-1}, f_\alpha\right)$$

$$= \int_{v>\hat{v}_+} P_R\left(v, f_\alpha\left(x,v\right)\right) |v-\hat{v}_+| q_B\left(H_B\left(v\right), f_{\alpha-1}\left(x,v\right)\right) \rho_{\alpha-1} \delta u_{\alpha-1}\left(v\right) \delta u_{\alpha-1}^+\left(\hat{v}_+\right) d\hat{v}_+$$

$$= \int_{v>\hat{v}_+} P_R\left(v, \rho_\alpha\right) |v-\hat{v}_+| q_B\left(H_B\left(v\right), \rho_{\alpha-1}\right) \rho_{\alpha-1} \delta u_{\alpha-1}\left(v\right) \delta u_{\alpha-1}^+\left(\hat{v}_+\right) d\hat{v}_+ \qquad (6)$$

(*b*) *Loss term to the left* (L_L^+) *defined as*:

$$L_L^+ (f_{\alpha-1}, f_\alpha, f_{\alpha+1})$$

$$= \int_{\hat{v}_- > v} P_L (v, \rho_{\alpha-1}) \left[1 - P_R \left(\hat{v}_-, \rho_{\alpha+1}\right)\right] |v - \hat{v}_-|$$

$$\times q_B \left(\hat{v}_-, \rho_\alpha\right) \rho_\alpha \delta u_\alpha^- \left(\hat{v}_-\right) \delta u_\alpha (v)\, d\hat{v}_- \tag{7}$$

Gain or Loss Due to Vehicles Acceleration

A vehicle will accelerate if the acceleration line is reached. Therefore:

(*a*) *Gain term from acceleration* (G_A^+) *is defined as:*

$$G_A^+ (f_\alpha) = \iint_{\hat{v}<\hat{v}_+} |\hat{v} - \hat{v}_+| \sigma_A \left(v, \hat{v}\right) q_A \left(H_A \left(\hat{v}\right), f_\alpha \left(x, \hat{v}\right)\right) \rho \delta u_\alpha \left(\hat{v}\right) \delta u_\alpha^+ \left(\hat{v}_+\right) d\hat{v} d\hat{v}_+$$

$$= \int \int_{\hat{v}<\hat{v}_+} |\hat{v} - \hat{v}_+| \sigma_A \left(v, \hat{v}_+\right) q_A \left(H_A \left(\hat{v}\right), \rho_\alpha\right) \rho_\alpha \delta u_\alpha \left(\hat{v}\right) \delta u_\alpha^+ \left(\hat{v}_+\right) d\hat{v} d\hat{v}_+ \tag{8}$$

(*b*) *Loss term from acceleration* (L_A^+) *is defined as*:

$$L_A^+ (f_\alpha) = \int_{v<\hat{v}_+} |v - \hat{v}_+| q_A \left(H_A (v), f_\alpha (x, v)\right) \rho_\alpha \delta u_\alpha (v)\, \delta u_\alpha^+ \left(\hat{v}_+\right) d\hat{v}_+$$

$$= \int_{v<\hat{v}_+} |v - \hat{v}_+| q_A \left(H_A (v), f_\alpha (x, v)\right) \rho_\alpha \delta u_\alpha (v)\, \delta u_\alpha^+ \left(\hat{v}_+\right) d\hat{v}_+ \tag{9}$$

Gain or Loss Due to Vehicles Deceleration

A vehicle will brake if it reaches the braking line and the driver is not able to change to the right or left lane. Therefore:

(*a*) *Gain term from braking interaction* (G_B^+) *is defined as*:

$$G_B^+ (f_{\alpha-1}, f_\alpha, f_{\alpha+1})$$

$$= \iint_{\hat{v}>\hat{v}_+} P_B \left(\hat{v}, \hat{v}_+, \rho_{\alpha-1}, \rho_{\alpha+1}\right) |\hat{v} - \hat{v}_+| \sigma_B \left(v, \hat{v}\right)$$

$$\times q_B \left(H_B \left(\hat{v}\right), \rho_\alpha\right) \rho_\alpha \delta u_\alpha \left(\hat{v}\right) \delta u_\alpha^+ \left(\hat{v}_+\right) d\hat{v} d\hat{v}_+ \tag{10}$$

(*b*) *Loss term from braking interaction* (L_B^+) *is defined as*:

$$L_B^+ (f_{\alpha-1}, f_\alpha, f_{\alpha+1})$$

$$= \int_{v>\hat{v}_+} P_B \left(v, \hat{v}_+, \rho_{\alpha-1}, \rho_{\alpha+1}\right) |v - \hat{v}_+| q_B \left(H_B (v), \rho_\alpha\right) \rho_\alpha \delta u_\alpha (v)\, \delta u_\alpha^+ \left(\hat{v}_+\right) d\hat{v}_+ \tag{11}$$

2.2. The Macroscopic Traffic Flow Model Equations

We use the method of moments to derive macroscopic equations from the kinetic equations above. To this end, we multiply the inhomogeneous kinetic equation (3) by v^k, $k = 0, 1$ and integrating it with respect to v in the range of $[0, v_{max}]$ to get the following set of balance equations;

$$\partial_t \int_0^{v_{max}} v^k f_\alpha (x, v, t)\, dv + \partial_x \int_0^{v_{max}} v^{k+1} f_\alpha (x, v, t)\, dv =$$

$$\int_0^{v_{max}} v^k \{\left(G_B^+ - L_B^+\right)(f_{\alpha-1}, f_\alpha, f_{\alpha+1}) + \left(G_A^+ - L_A^+\right) f_\alpha$$

$$+ \left[G_R^+ (f_\alpha, f_{\alpha+1}, f_{\alpha+2}) - L_R^+ (f_\alpha, f_{\alpha+1})\right]$$

$$+ \left[G_L^+ (f_{\alpha-1}, f_\alpha) - L_L^+ (f_{\alpha-1}, f_\alpha, f_{\alpha+1})\right]\} dv \tag{12}$$

Considering the Gain and Loss terms interactions due to lane changing, acceleration and braking and applying the Dirac delta (δ) function in the sense of distribution, Kimathi [10], we combine equations (6) and (7) to get:

$$\int_0^{v_{max}} v^k \left[G_L^+ (f_{\alpha-1}, f_\alpha) - L_L^+ (f_{\alpha-1}, f_\alpha, f_{\alpha+1})\right] dv$$

$$= \left[\rho_{\alpha-1} u_{\alpha-1}^k |u_{\alpha-1} - u_{\alpha-1}^+| P_R (u_{\alpha-1}, \rho_\alpha)\, q_B (H_B (u_{\alpha-1}), \rho_{\alpha-1})\right]$$

$$-\rho_\alpha u_\alpha^k |u_\alpha - u_\alpha^-| P_L (u_\alpha, \rho_{\alpha-1}) \left(1 - P_R \left(u_\alpha^-, \rho_{\alpha+1}\right)\right) q_B \left(H_B(u_\alpha^-), \rho_\alpha\right) \tag{13}$$

similarly equations (4) and (5) give:

$$\int_0^{v_{max}} v^k \left[G_R^+ (f_\alpha, f_{\alpha+1}, f_{\alpha+2}) - L_R^+ (f_\alpha, f_{\alpha+1})\right] dv$$

$$= \rho_{\alpha+1} u_{\alpha+1}^k |u_{\alpha+1} - u_{\alpha+1}^-| P_L (u_{\alpha+1}, \rho_\alpha) \left[1 - P_R \left(u_{\alpha+1}^-, \rho_{\alpha+2}\right)\right] q_B \left(H_B(u_{\alpha+1}^-), \rho_{\alpha+1}\right)$$

$$-\rho_\alpha u_\alpha^k |u_\alpha - u_\alpha^+| P_R (u_\alpha, \rho_{\alpha+1})\, q_B (H_B (u_\alpha), \rho_\alpha) \tag{14}$$

Combining equations (8) and (9), we get;

$$\int_0^{v_{max}} v^k \left(G_A^+ - L_A^+\right) f_\alpha dv$$

$$\simeq \rho_\alpha h_A q_A \left(H_A\left(u_\alpha\right), \rho_\alpha\right) \frac{\eta-1}{2} u_\alpha \partial_x u_\alpha \tag{15}$$

similarly equations (10) and (11) give:

$$\int_0^{v_{max}} v^k \left(G_B^+ - L_B^+\right)\left(f_{\alpha-1}, f_\alpha, f_{\alpha+1}\right) dv$$

$$\simeq \rho_\alpha h_B P_B\left(u_\alpha, u_\alpha^+, \rho_{\alpha-1}, \rho_{\alpha+1}\right) q_B\left(H_B\left(u_\alpha\right), \rho_\alpha\right) \frac{1-\beta}{2} u_\alpha \partial_x u_\alpha \tag{16}$$

For equations (15) and (16), we assume that the leading vehicles are distributed in such a way that;

$$h_B q_B\left(H_B(u_\alpha), \rho_\alpha\right) = h_A q_A\left(H_A(u_\alpha), \rho_\alpha\right) = \frac{db\left(\rho_\alpha\right)}{d\rho_\alpha} \tag{17}$$

with $b\left(\rho_\alpha\right)$ being some increasing function of density ρ_α, [10] . Therefore the anticipation term is deduced from (15) and (16) using (17), and is written as;

$$a\left(\rho_\alpha, u_\alpha\right) = \begin{cases} \rho_\alpha \dfrac{db\left(\rho_\alpha\right)}{d\rho_\alpha} \varphi_B\left(u_\alpha, u_\alpha^+, \rho_{\alpha-1}, \rho_{\alpha+1}\right), & \partial_x u_\alpha < 0 \\ \rho_\alpha \dfrac{db\left(\rho_\alpha\right)}{d\rho_\alpha} \varphi_A\left(u_\alpha\right), & \partial_x u_\alpha > 0 \end{cases} \tag{18}$$

where $\varphi_A\left(u_\alpha\right) = \dfrac{(\eta-1)}{2} u_\alpha$ and

$$\varphi_B\left(u_\alpha, u_\alpha^+, \rho_{\alpha-1}, \rho_{\alpha+1}\right) = P_B\left(u_\alpha, u_\alpha^+, \rho_{\alpha-1}, \rho_{\alpha+1}\right)\left(\frac{1-\beta}{2}\right) u_\alpha$$

Assuming that for $\partial_x u_\alpha < 0$, braking is inevitable i.e. $P_B\left(u_\alpha, u_\alpha^+, \rho_{\alpha-1}, \rho_{\alpha+1}\right)$ approaches one and taking $\dfrac{(\eta-1)}{2} u_\alpha \simeq C$, then;

$$a\left(\rho_\alpha\right) = \rho_\alpha \frac{db\left(\rho_\alpha\right)}{d\rho_\alpha} C \tag{19}$$

Using the following specifications of probabilities approximation,

$$P_Y\left(u_\alpha, \rho_\alpha\right) \sim exp\left(-\rho_\alpha \phi\left(u_\alpha\right)\right) = e^{-\rho_\alpha \phi\left(u_\alpha\right)}$$

$$q_X\left(H_B\left(u_\alpha\right), \rho_\alpha\right) \sim \frac{1}{1-\rho_\alpha}$$

and taking $\phi\left(u_\alpha\right) \sim C_0$, the right hand side of equation (13) becomes; for k=0,1:

$$\Phi_1^0\left(\alpha-1, \alpha, \alpha+1\right)$$

$$= \rho_{\alpha-1}|u_{\alpha-1} - u_{\alpha-1}^{+}|e^{-\rho_\alpha C_0}\left(\frac{1}{1-\rho_{\alpha-1}}\right)$$

$$-\rho_\alpha|u_\alpha - u_\alpha^{-}|e^{-\rho_{\alpha-1}C_0}\left(1-e^{-\rho_{\alpha+1}C_0}\right)\left(\frac{1}{1-\rho_\alpha}\right) \tag{20}$$

$$\Phi_1^1\left(\alpha-1,\alpha,\alpha+1\right)$$

$$= \rho_{\alpha-1}u_{\alpha-1}|u_{\alpha-1} - u_{\alpha-1}^{+}|e^{-\rho_\alpha C_0}\left(\frac{1}{1-\rho_{\alpha-1}}\right)$$

$$-\rho_\alpha u_\alpha|u_\alpha - u_\alpha^{-}|e^{-\rho_{\alpha-1}C_0}\left(1-e^{-\rho_{\alpha+1}C_0}\right)\left(\frac{1}{1-\rho_\alpha}\right) \tag{21}$$

Similarly for $k = 0, 1$ the right hand side of equation (14) becomes:

$$\Phi_2^0\left(\alpha,\alpha+1,\alpha+2\right)$$

$$= \rho_{\alpha+1}|u_{\alpha+1} - u_{\alpha+1}^{-}|e^{-\rho_\alpha C_0}\left(\frac{1}{1-\rho_{\alpha+1}}\right)$$

$$\times\left(1-e^{-\rho_{\alpha+2}C_0}\right) - \rho_\alpha|u_\alpha - u_\alpha^{+}|e^{-\rho_{\alpha+1}C_0}\left(\frac{1}{1-\rho_\alpha}\right) \tag{22}$$

$$\Phi_2^1\left(\alpha,\alpha+1,\alpha+2\right)$$

$$= \rho_{\alpha+1}u_{\alpha+1}|u_{\alpha+1} - u_{\alpha+1}^{-}|e^{-\rho_\alpha C_0}\left(\frac{1}{1-\rho_{\alpha+1}}\right)$$

$$\times\left(1-e^{-\rho_{\alpha+2}C_0}\right) - \rho_\alpha u_\alpha|u_\alpha - u_\alpha^{+}|e^{-\rho_{\alpha+1}C_0}\left(\frac{1}{1-\rho_\alpha}\right) \tag{23}$$

Taking $f_\alpha\left(x,v,t\right) = \rho_\alpha \delta u_\alpha\left(v\right)$, then the left hand side of equation (12) becomes:

$$\partial_t \int_0^{v_{max}} v^k \rho_\alpha \delta u_\alpha\left(v\right) dv + \partial_x \int_0^{v_{max}} v^{k+1} \rho_\alpha \delta u_\alpha\left(v\right) dv$$

Thus for $k = 0$, then:

$$\partial_t \rho_\alpha + \partial_x(\rho_\alpha u_\alpha) = \Phi_1^0\left(\alpha-1,\alpha,\alpha+1\right) + \Phi_2^0\left(\alpha,\alpha+1,\alpha+2\right) \tag{24}$$

and for $k = 1$,

$$\partial_t(\rho_\alpha u_\alpha) + \partial_x(\rho_\alpha u_\alpha^2) - a\left(\rho_\alpha\right)\partial_x u_\alpha$$

$$= \Phi_1^1\left(\alpha-1,\alpha,\alpha+1\right) + \Phi_2^1\left(\alpha,\alpha+1,\alpha+2\right) \tag{25}$$

Where $a\left(\rho_\alpha\right)$ is the anticipation term from drivers due to speed adaptation effect.

Equations (24) and (25) are the derived macroscopic traffic flow model of Aw-Rascle type.

2.3. The Relaxation Term

In order to reproduce the traffic breakdown that occurs at the bottlenecks such as on-ramp, according to the empirical studies done by Kerner [1], we introduce a relaxation term to the velocity dynamics equation (25) as specified in [10]. It is through this relaxation term that Kerner's hypothesis of 3-phase traffic flow can also be incorporated into our model for multi-lane traffic flow. The relaxation term $R(\rho_\alpha, u_\alpha)$ considered for this study is specified as follows:

$$R(\rho_\alpha, u_\alpha) = \frac{1}{T}\left(U_\alpha^e(\rho_\alpha, u_\alpha) - u_\alpha\right) \tag{26}$$

where

$$U_\alpha^e(\rho_\alpha, u_\alpha) = \begin{cases} u_1^e(\rho_\alpha), & \rho_\alpha < \rho_{\alpha,min}^{syn},\ or\ u_\alpha > R(\rho_\alpha),\ \rho_{\alpha,min}^{syn} < \rho_\alpha < \rho_{\alpha,max}^{free} \\ u_2^e(\rho_\alpha), & u_\alpha < R(\rho_\alpha),\ \rho_{\alpha,min}^{syn} < \rho_\alpha < \rho_{\alpha,max}^{free},\ or\ \rho_\alpha > \rho_{\alpha,max}^{free} \end{cases} \tag{27}$$

$u_1^e(\rho_\alpha)$ and $u_2^e(\rho_\alpha)$ are two optimal velocity curves defined in [10] such that $u_2^e(\rho_\alpha) < u_1^e(\rho_\alpha)$, $0 \le \rho_\alpha < \rho_{\alpha,max}$ with $u_1(\rho_{\alpha,max}) = u_2(\rho_{\alpha,max}) = 0$ and are monotone decreasing functions of density satisfying the property; $u_1^e(\rho_\alpha) > R(\rho_\alpha) > u_2^e(\rho_\alpha)$, $\rho_{\alpha,min}^{syn} < \rho_\alpha < \rho_{\alpha,max}^{free}$
with $u_2^e\left(\rho_{\alpha,min}^{syn}\right) = R\left(\rho_{\alpha,min}^{syn}\right)$, $u_1^e\left(\rho_{\alpha,max}^{free}\right) = R\left(\rho_{\alpha,max}^{free}\right)$. Here $\rho_{\alpha,min}^{syn}$ is the minimum density below which synchronized flow cannot occur, $\rho_{\alpha,max}^{free}$ is the limit density for free flow existence and $R(\rho_\alpha)$ is a switching curve viewing the traffic dynamics from the density perspective. The curve $u_1^e(\rho_\alpha)$ characterize the fast mode where the traffic is less dense and allow easy lane change and overtaking manoeuvres. The curve $u_2^e(\rho_\alpha)$ characterize the slower mode, where the traffic is more dense and give a lesser chance of lane change and overtaking manoeuvres. Therefore equation (25) is written as;

$$\begin{aligned} \partial_t(\rho_\alpha u_\alpha) + \partial_x(\rho_\alpha u_\alpha^2) - a(\rho_\alpha)\,\partial_x u_\alpha = {} & \rho_\alpha R(\rho_\alpha, u_\alpha) + \Phi_1^1(\alpha-1, \alpha, \alpha+1) \\ & + \Phi_2^1(\alpha, \alpha+1, \alpha+2) \end{aligned} \tag{28}$$

2.4. Numerical Simulations

We consider a highway with three lanes and an on-ramp as the bottleneck for our traffic simulations as shown in the figure 2.

For a proper numerical approximation, equations (24) and (28) can be cast into:

$$\partial_t U_\alpha + \partial_x F(U_\alpha) = S(U_\alpha) \tag{29}$$

Where $U_\alpha = (\rho_\alpha, \rho_\alpha u_\alpha + \rho_\alpha p(\rho_\alpha))^T$, $F(U_\alpha) = (\rho_\alpha u_\alpha, \rho_\alpha u_\alpha(u_\alpha + p(\rho_\alpha)))^T$ and $S(U_\alpha) = (\rho_\alpha u_\alpha, \rho_\alpha u_\alpha(u_\alpha + p(\rho_\alpha)))^T$ are vectors of conserved variables, fluxes and the source term respectively.

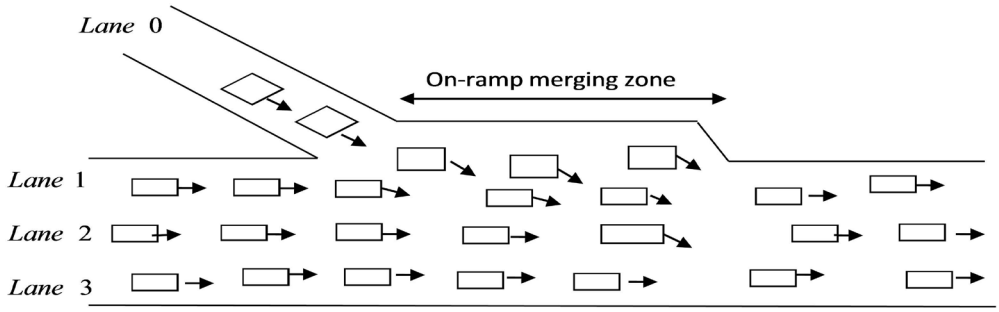

Figure 2: Section of the highway with three lanes and an on-ramp.

Given that the general initial data for the homogeneous system of equation below

$$\partial_t U_\alpha + \partial_x F\left(U_\alpha\right) = 0 \tag{30}$$

is $\widetilde{U}_\alpha\left(x, t^n\right)$, we evolve the solution to a time step $t^{n+1} = t^n + \triangle t$ by use of the Godunov method in the following steps:

- At first we assume a piecewise constant distribution of data by defining cell averages as;

$$U^n_{\alpha,i} = \frac{1}{\triangle x}\int_{x-\frac{1}{2}}^{x+\frac{1}{2}} \widetilde{U}_\alpha\left(x, t^n\right) dx \tag{31}$$

Then we discretize the spatial domain into M cells, $C_i = \left[x_{i-\frac{1}{2}}, x_{i+\frac{1}{2}}\right]$ for $i = 1, \ldots, M$ of the same size $\triangle x$. These cell averages produce the required piecewise constant distribution $U_\alpha\left(x, t^n\right) = U^n_{\alpha,i}$ data now consist of the set of values $\left\{U^n_{\alpha,i}\right\}$.

- For the rectangular control volume $\left[x_{i-\frac{1}{2}}, x_{i+\frac{1}{2}}\right] \times \left[t^n, t^{n+1}\right]$ shown in figure 3.

We obtain the required Godunov numerical scheme as:

$$U^{n+1}_{\alpha,i} = U^n_{\alpha,i} + \frac{\triangle t}{\triangle x}\left[F(U^n_{\alpha,i-\frac{1}{2}}(0)) - F(U^n_{\alpha,i+\frac{1}{2}}(0))\right] \tag{32}$$

Remark 2.2. In order to contain the interactions of the waves within the cell C_i during the calculations, we impose the Courant-Friedrichs-Lewy restriction (*CFL condition*) on time step size $\triangle t$ as;

$$\triangle t \leq \frac{C_{cfl}\triangle x}{Max\left\{\ |\lambda_i\left(U_\alpha\right)|,\ \ i = 1, 2\ \right\}} \tag{33}$$

where $C_{cfl} \leq 1$, a constant called the Courant number. This is a condition for numerical stability where a numerical solution is unstable if the errors grow exponentially, which in turn may lead to oscillation of traffic variables with very short wavelength.

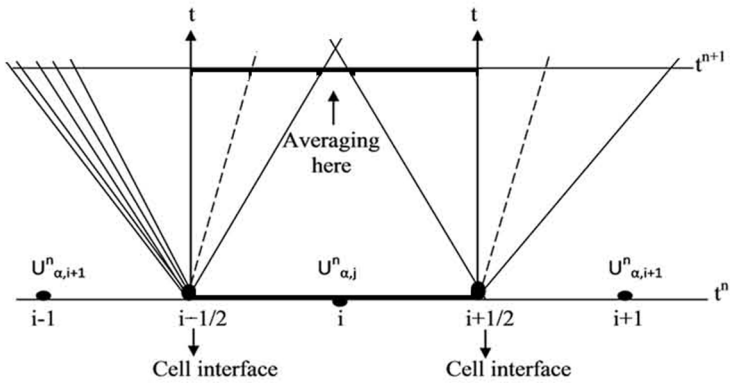

Figure 3: Typical rectangular control volume.

In order to proceed with simulation of our traffic flow features, we introduce the source term $S(U_\alpha)$ to the right hand side of the conservative system of equation (30). The following approximations are used to obtain the equations below;

$$u_\alpha^+(x,t) \simeq u_\alpha(i+1,k)$$

and

$$u_\alpha^-(x,t) \simeq u_\alpha(i-1,k)$$

a) For lane 1, i.e when $\alpha = 1$, equations (20),(21),(22) and (23) respectively becomes;

$$\Phi_1^0(0,1,2) \simeq \rho_0(i,k)\,|u_0(i,k) - u_0(i+1,k)\,|e^{-\rho_1(i,k)C_0}\left(\frac{1}{1-\rho_0(i,k)}\right) \tag{34}$$

$$\Phi_1^1(0,1,2) \simeq \rho_0(i,k)\,u_0(i,k)\,|u_0(i,k) - u_0(i+1,k)\,|e^{-\rho_1(i,k)C_0}\left(\frac{1}{1-\rho_0(i,k)}\right) \tag{35}$$

$$\Phi_2^0(1,2,3) \simeq \rho_2(i,k)\,|u_2(i,k) - u_2(i-1,k)\,|e^{-\rho_1(i,k)C_0}\left(\frac{1}{1-\rho_2(i,k)}\right)$$

$$\times\left(1-e^{-\rho_3(i,k)C_0}\right) - \rho_1(i,k)\,|u_1(i,k) - u_1(i+1,k)\,|e^{-\rho_2(i,k)C_0}\left(\frac{1}{1-\rho_1(i,k)}\right) \tag{36}$$

$$\Phi_2^1(1,2,3) \simeq \rho_2(i,k)\,u_2(i,k)\,|u_2(i,k) - u_2(i-1,k)\,|e^{-\rho_1(i,k)C_0}\left(\frac{1}{1-\rho_2(i,k)}\right)$$

$$\times\left(1-e^{-\rho_3(i,k)C_0}\right) - \rho_1(i,k)\,u_1(i,k)\,|u_1(i,k) - u_1(i+1,k)\,|e^{-\rho_2(i,k)C_0}\left(\frac{1}{1-\rho_1(i,k)}\right) \tag{37}$$

b) For lane 2, i.e when $\alpha = 2$, equations (20),(21),(22) and (23) respectively becomes;

$$\Phi_1^0(1,2,3) \simeq \rho_1(i,k)\,|u_1(i,k) - u_1(i+1,k)\,|e^{-\rho_2(i,k)C_0}\left(\frac{1}{1-\rho_1(i,k)}\right)$$

$$-\rho_2(i,k)\,|u_2(i,k) - u_2(i-1,k)\,|e^{-\rho_1(i,k)C_0}\left(1-e^{-\rho_3(i,k)C_0}\right)\left(\frac{1}{1-\rho_2(i,k)}\right) \quad (38)$$

$$\Phi_1^1(1,2,3) \simeq \rho_1(i,k)\,u_1(i,k)\,|u_1(i,k) - u_1(i+1,k)\,|e^{-\rho_2(i,k)C_0}\left(\frac{1}{1-\rho_1(i,k)}\right)$$

$$-\rho_2(i,k)\,u_2(i,k)\,|u_2(i,k) - u_2(i-1,k)\,|e^{-\rho_1(i,k)C_0}\left(1-e^{-\rho_3(i,k)C_0}\right)\left(\frac{1}{1-\rho_2(i,k)}\right) \quad (39)$$

$$\Phi_2^0(2,3,4) \simeq \rho_3(i,k)\,|u_3(i,k) - u_3(i+1,k)\,|e^{-\rho_2(i,k)C_0}\left(\frac{1}{1-\rho_3(i,k)}\right)$$

$$-\rho_2(i,k)\,|u_2(i,k) - u_2(i-1,k)\,|e^{-\rho_3(i,k)C_0}\left(\frac{1}{1-\rho_2(i,k)}\right) \quad (40)$$

$$\Phi_2^1(2,3,4) \simeq \rho_3(i,k)\,u_3(i,k)\,|u_3(i,k) - u_3(i+1,k)\,|e^{-\rho_2(i,k)C_0}\left(\frac{1}{1-\rho_3(i,k)}\right)$$

$$-\rho_2(i,k)\,u_2(i,k)\,|u_2(i,k) - u_2(i-1,k)\,|e^{-\rho_3(i,k)C_0}\left(\frac{1}{1-\rho_2(i,k)}\right) \quad (41)$$

c) For lane 3, i.e when $\alpha = 3$ equations (20),(21),(22) and (23) respectively becomes;

$$\Phi_1^0(2,3,4) \simeq \rho_2(i,k)\,|u_2(i,k) - u_2(i+1,k)\,|e^{-\rho_3(i,k)C_0}\left(\frac{1}{1-\rho_2(i,k)}\right)$$

$$-\rho_3(i,k)\,|u_3(i,k) - u_3(i-1,k)\,|e^{-\rho_2(i,k)C_0}\left(\frac{1}{1-\rho_3(i,k)}\right) \quad (42)$$

$$\Phi_1^1(2,3,4) \simeq \rho_2(i,k)\,u_2(i,k)\,|u_2(i,k) - u_2(i+1,k)\,|e^{-\rho_3(i,k)C_0}\left(\frac{1}{1-\rho_2(i,k)}\right)$$

$$-\rho_3(i,k)\,u_3(i,k)\,|u_3(i,k) - u_3(i-1,k)\,|e^{-\rho_2(i,k)C_0}\left(\frac{1}{1-\rho_3(i,k)}\right) \quad (43)$$

3. Results and Discussion

Let the highway under consideration be along the x-axis; where $x = -30$ is the distance upstream of the bottleneck, $x = 0$ is the location of the bottleneck and $x = 10$ is the distance downstream of the bottleneck. Let the flow of traffic be in the direction of increasing x along the axis and $t \in [0, 500]$ be the time interval of the traffic simulation.

Figure 4 and 5 show the simulations of the observed features of spatiotemporal congested traffic patterns that occur in the vicinity of the on-ramp bottleneck. After traffic breakdown occur at the on-ramp, various congested patterns of synchronized flow are observed upstream and downstream of the bottleneck, see figure 4 and 5. From these patterns, it is observed that congestion in lane 1 begins immediately after the vehicles from the on-ramp merge on to the highway which then begins propagating upstream. The congestion sets into lane 1 because the vehicles in this lane slow down to give way to those merging from the on-ramp. This happens frequently during rush hours causing traffic to build up on lane 1 from the on-ramp location towards the upstream direction.

Table 1: Model parameters used in simulations

Parameters	**Values**	**Parameters**	**Values**
$C = c_0$	0.45	$\rho_{\alpha,min}^{syn}$	0.5
C_{cfl}	0.5	$\rho_{\alpha,max}^{free}$	0.3
$\rho_{\alpha,jam}$	0.9		

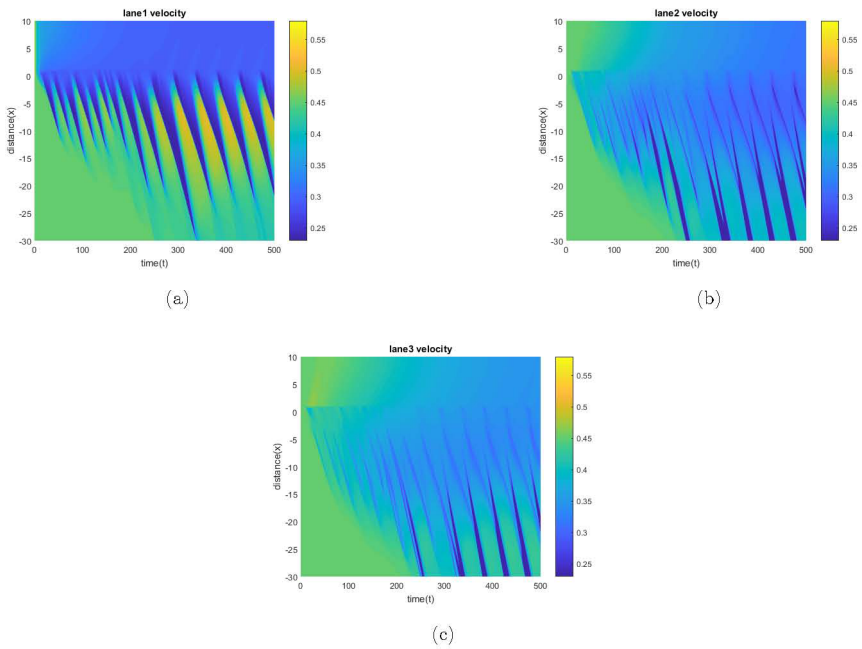

Figure 4: Velocity space - time traffic patterns of the lanes 1, 2 and 3 near the on-ramp.

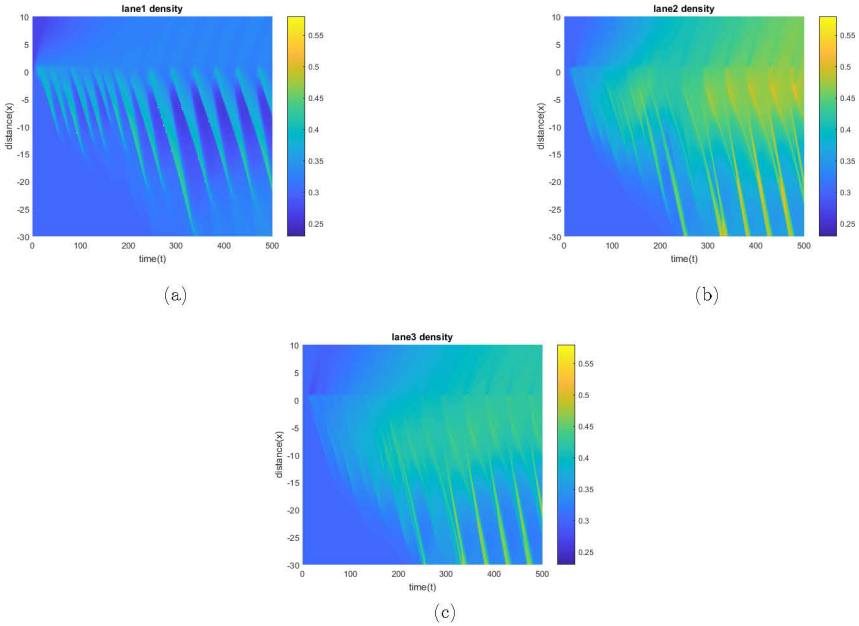

Figure 5: Density Space-time traffic patterns of the lanes 1, 2 and 3 near the on-ramp

Hence a stop-and-go traffic pattern is formed as depicted in figure 4(a). After sometimes, the traffic flow in lanes 2 and 3 are also affected by the aggressive drivers in lane 1 who upon experiencing or anticipating the constrainedness opt to improve or maintain their driving conditions by changing lane to these lanes. Due to the traffic disturbance caused by the on-ramp inflow rate (q_{on}) and more vehicles in lane 1 changing lane to lanes 2 and 3, there is an increase in vehicle density and a decrease in vehicle velocity in lane 2 and 3 upstream of the bottleneck. Figure 4 (b) shows that there is a tendency towards synchronization of vehicles speeds on the highway at the bottleneck indicated by region of fluctuating average low velocities. In lane 2 and 3, a moving synchronized pattern (MSP) appears on the highway upstream of the on-ramp. Thus the two lanes (2 and 3) experience traffic congestion upstream of the bottleneck where the traffic queue grow at the tail while the vehicles at the head of the queue accelerate as shown in figure 4 and 5. However, in the three lanes downstream of the on-ramp, there is an immediate decrease in both velocity and density showing that few vehicles are able to manoeuvre out of the traffic merging region. Therefore, there is free flow downstream after the merging zone in the three lanes where the vehicles have to over-accelerate.

Figure 6a,b and c shows the traffic flow-density relationship in the three lanes, where in lane 1 there is a decrease in flow rate within the deterministic disturbance as the vehicle density increases at the on-ramp ($x = 0$) . It is observed that congestion in lane 1 occurs when the vehicles from on-ramp lane 0 merge with the vehicles in that lane at the bottleneck. Consequently, the aggressive drivers in lane 1 opt to change lanes to the faster ones immediately they approach the traffic merging region. The flow rate in lanes 2 and 3 is sustained at the bottleneck ($x = 0$), see figure 6b and 6c. This implies that at

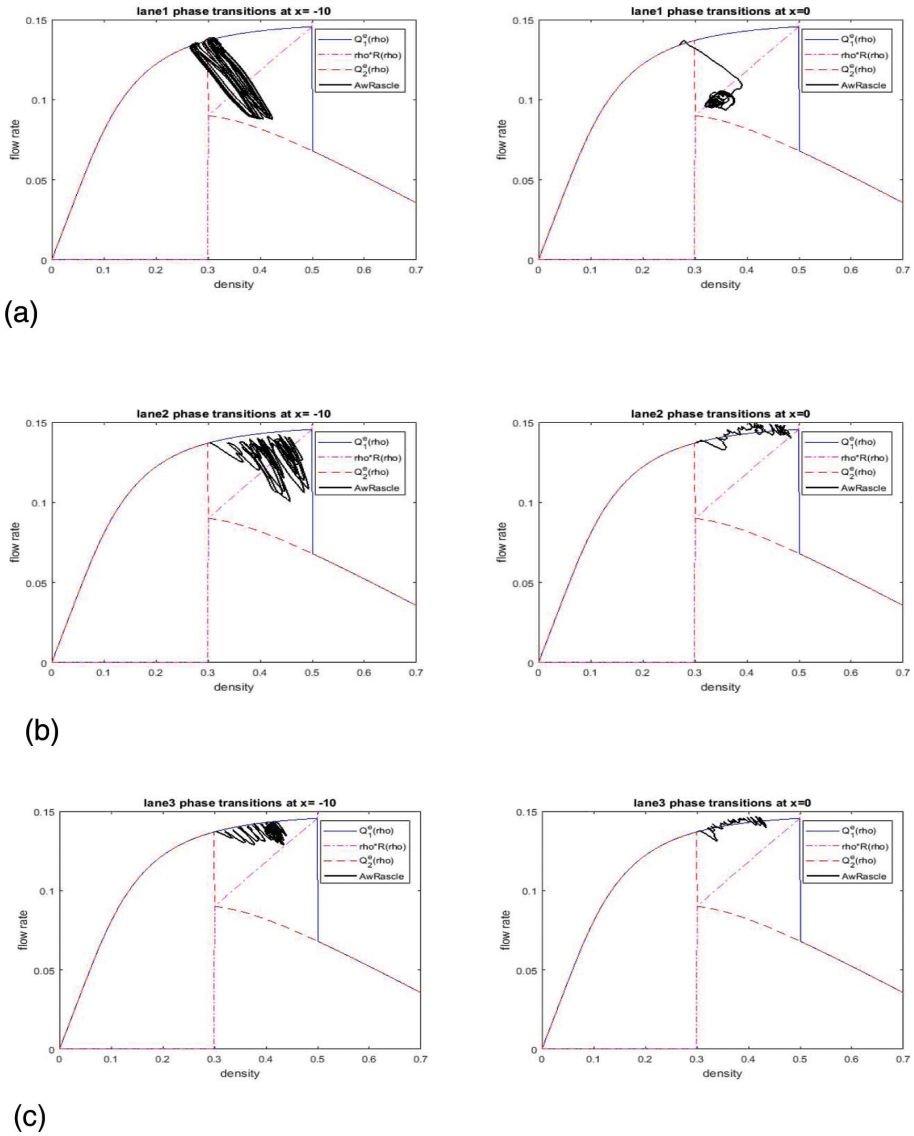

Figure 6: (a) Traffic flow rate-density relationship in lane 1 at location $x = 0$ and $x = -10$. (b) Traffic flow rate-density relationship in lane 2 at location $x = 0$ and $x = -10$. (c) Traffic flow rate-density relationship in lanes 3 at location $x = 0$ and $x = -10$.

the bottleneck, most vehicles on the highway prefer to move in lanes 2 and 3 than in lane 1 as long as possible to avoid the vehicles merging onto the highway from on-ramp. At location ($x = -10$) upstream of the bottleneck, there is a random fluctuation in flow rate with increase of traffic density as shown in figure 6 that is, maximum flow rate is attained at low density and vice versa. This traffic flow situation is short lived since vehicles are interacting by changing lanes from lane 1 to the right lanes in the vicinity of an on-ramp. Therefore a transition of free flow to synchronized flow ($F \rightarrow S$) occurs (where the flow

rate is high and the average velocity is low). This ($F \rightarrow S$) transition last for only a short period and transition from synchronized to free flow ($S \rightarrow F$) appear. Thus, the traffic phase transition exchange is continuous at this location and complete a traffic hysteresis loop, in which the upper part of the loop represents the vehicle deceleration branch in ($F \rightarrow S$) transition while the lower part of the loop is the acceleration branch associated with ($S \rightarrow F$).

4. Conclusion

A multi-lane macroscopic traffic flow model of Aw-Rascle type within the framework of the 3-phase traffic flow theory of Kerner has been derived. This has been achieved by applying the method of moments on the kinetic traffic flow model where we obtained the kinetic interaction operators (gain and loss terms). For simulation of our traffic congestion, we have considered a highway with three lanes and an on-ramp. Finite volume method (Godunov scheme) was used to compute the numerical solutions for our traffic flow model equations. The discretized form of the source term equations are obtained for the three lanes in highway and solved using Euler's method. With these simulations near an on-ramp, the derived macroscopic traffic flow model is able to reproduce the spatiotemporal features of real traffic flow near the bottleneck. The simulations show that the initial traffic flow disturbance occurs only in the lane adjacent to the on-ramp due to the merging of vehicles from on-ramp. However the disturbance can grow leading to a transition from a free flow to synchronized one,in particular when the vehicle lane-changes leads to the deceleration of the following vehicles in the target lanes. Therefore vehicles lane-change manoeuvre in the vicinity of an on-ramp can lead to traffic congestion. This study indicates that the macroscopic multi-lane traffic flow model derived above can be used to;

- improve the design and safety of roads by identifying the effective location of the bottlenecks to evaluate the impact of new road infrastructure
- solve road congestion problems by either erecting traffic control lights or use the traffic marshals / policemen to control the traffic jam in the vicinity of the highway bottlenecks
- explain and predict when the traffic jams will emerge at the highway bottlenecks

Recommendations

In this work, a macroscopic traffic flow model has been developed with traffic simulations done in the vicinity of an on-ramp bottlenecks. It is recommended that further simulations of traffic congestion due to an off-ramp be carried out, and a comparison of these effects with those of an on-ramp be done.

References

[1] Kerner, B.S, *Introduction to Modern Traffic Flow Theory and Control*. The long road to three-phase traffic theory, Springer, first edition, 2009.

[2] Whitman, G, *Linear and Nonlinear Waves.* Wiley, New York, 1974.

[3] Payne, H. and Freflo, *A Macroscopic Simulation Model of Freeway Traffic.* Transportation Research Record 722, pp. 68–75, 1979.

[4] Daganzo, C. F, Requiem for Second Order Fluid Approximations of Traffic Flow. *Transportation Research* B29(4), pp. 227–286, 1995.

[5] Aw, A. and Rascle, M, Resurrection of "Second Order" Models of Traffic Flow. *SIAM Journal on Applied Mathematics* 60(5), pp. 916–938, 2000.

[6] Klar, A. and Wegener, R, A Hierarchy of Models for Multilane Vehicular Traffic modeling. *SIAM Journal on Applied Mathematics* 59(4), pp. 983–1001, 1998.

[7] Ahmed, K. I, *Modeling Driver's Acceleration and Lane Changing Behavior.* PhD Thesis, Massachusetts Institute of Technology, U.S.A, 1999.

[8] Hoogendoorn, S. P, *Multiclass Continuum Modeling of Multilane Traffic Flow*. PhD Thesis, Delft University of Technology, Netherlands, 1999.

[9] Helbing, D., Johansson, A. F, On the Controversy Around Daganzo's Requiem for and Aw-Rascle's Resurrection of Second-Order Traffic Flow Models. *European Physical Journal* B 69(4), pp. 549–562, 2009.

[10] Kimathi, E. M, *Mathematical Models for 3-phase Traffic Flow Theory.* PhD Thesis, Technical University of Kaiserslautern, Germany, 2012.